AAS 20-625

# THREE SATELLITES FORMATION FLYING: DEPLOYMENT AND FORMATION ACQUISITION USING RELATIVE ORBITAL ELEMENTS.

**Francesca Scala[*], Gabriella Gaias[†], Camilla Colombo[‡], and Manuel Martin-Neira[§]**

This paper presents the analysis for the deployment and the acquisition procedures for a three-satellites formation flying, on a sun-synchronous orbit, as part of a study for a European Space Agency potential high resolution L-band radiometer mission for land and ocean applications. The methodologies for formation-flight establishment and reconfiguration maneuvers are presented, to enable the operational phase which foresees a continuous low-thrust control profile to keep the formation rigid and safe. The design is performed using relative orbital elements, including maximum delta-v limitation, safety condition requirements, and perturbation effects. The results, verified through high-fidelity propagation, apply to a wide range of Earth observation missions exploiting distributed systems.

## INTRODUCTION

In the last decade, multi-satellite formation flying missions have increased their importance in the field of Earth observation and remote sensing. Distributed missions, where different satellites work as distributed nodes of a network of sensors, can enhance the capabilities of a single spacecraft, both for scientific performances and single-point failure risk.[1,2] Since 2009, the Soil Moisture and Ocean Salinity (SMOS) satellite has shown how high-resolution scientific observations could improve the performances of a wide range of land and ocean applications, such as meteorological and climate predictions.[3,4] Exploiting multi-satellite formation flying is seen as a potential opportunity to increase the virtual aperture size of the scientific payloads, and, as a result, their spatial resolution.[5,6] This paper presents the analysis for the deployment and the formation acquisition procedures for a three-satellites formation flying, on a perturbed quasi-circular Sun-Synchronous orbit at 770 km of altitude. Specifically, this study is part of a new mission concept proposed by the European Space Agency (ESA) devoted to the investigation of the feasibility of future multi-satellite formation-flying for L-band interferometry applications. Given the current capabilities of distributed systems, the possibility to deploy a formation of three identical satellites is envisioned, mounting an L-band interferometric radiometer for scientific purposes. A preliminary study on the scientific payload demonstrated the feasibility to achieve a spatial resolution of 1-10 km for land and oceans application, instead of the 40 km resolution of the SMOS single-satellite mission.[3,6,7]

[*]Ph.D. student, Department of Aerospace Science and Technology, Politecnico di Milano, 20156, Milano, Italy.
[†]Research Engineer, Department of Aerospace Science and Technology, Politecnico di Milano, 20156, Milano, Italy.
[‡]Associate Professor, Department of Aerospace Science and Technology, Politecnico di Milano, 20156, Milano, Italy.
[§]Technical officer Engineer, European Space Agency, ESA-ESTEC, 2200 AG, Noordwijk, The Netherlands.

The design of the initial phase of the mission is important for formation flying missions. Ensuring collision avoidance during the formation deployment is very challenging and requires the selection of proper initial safe separation conditions.[8] For the case in analysis, the formation will be placed with a single launch on a Sun-Synchronous Orbit (SSO). The deployment mechanism will impart a separation velocity to each of the three satellites. The analysis is performed in the framework of the Relative Orbital Elements (ROEs),[9,10] as well as considering the shape of the relative trajectories in the co-moving radial-transversal-normal (RTN) orbital frame.[11,12] During the commissioning phase of each satellite, the most relevant perturbations in the low Earth orbit environment are included. For design purposes, a clear insight can be gained using the analytical first-order state transition matrix and second-order state transition tensor of the relative dynamics, subject to the perturbation from the whole geopotential.[10] The major contribution – produced by the Earth's oblateness $J_2$ - causes a secular drift in some ROEs, and this behavior must be carefully considered to ensure that the relative motion remains in the required boundary, with no collision risk probability.

This paper presents the maneuvers strategy for an optimal formation reconfiguration before the nominal scientific operations begin. In literature, the problems of formation reconfiguration have been widely studied. Several solutions have been proposed for either impulsive or continuous control. The former is typically preferred with stringent payload constraint, which might require a reduction of the disturbances due to a continuous thrust profile.[13–15] Conversely, the latter thrust profile can generate continuously a very precise output for the formation maintenance and correction of relative navigation errors.[16–18]

For the mission presented, the L-band scientific payloads require a fixed relative attitude profile for proper functioning. A continuous control profile is required during the nominal scientific phase to keep a rigid formation and a safe flight condition. Accordingly, the propulsion system embarked on the spacecraft has been sized to enable such specific baseline formation. Consequently, the authors investigate continuous thrust reconfiguration strategies for establishing the nominal formation geometry. The relative motion of the satellites is described in both the ROEs framework and in the RTN orbital frame. The system dynamics include the effect of the $J_2$ perturbation, which is the most relevant perturbing term to the unperturbed motion for the case under study. Moreover, the continuous thrust profile is included as an acceleration contribution to the natural motion. The aim of the reconfiguration maneuver is the design of the optimal trajectory for the formation, which minimizes the propellant consumption and implements the collision-avoidance conditions. The optimization procedure can be addressed with different strategies. This paper presents an optimization technique that relies on convex optimization.[19] Such procedure allows the computation of the optimal condition with low computational cost, by solving a convex minimization problem. For this reason, the strategy could also be considered to be implemented on-board for real-time computation of generic reconfiguration maneuvers for the formation, during the operational life of the mission.[17]

The proposed analysis provides a baseline procedure to safely initialize the formation and to define the requirements for the deployment system of the launcher. The methodology applies to other multi-satellite missions in similar orbital scenarios, also considering the recent trend of employing low-thrust engines on-board scientific satellites. The results of this analysis are verified through high-fidelity simulations to assess the realistic performances of the proposed guidance and control strategies.

## MISSION OVERVIEW

The mission presented is a Formation Flying (FF) study currently in development by the European Space Agency, Airbus, and Politecnico di Milano, intending to increase the imaging resolution by exploiting the virtual aperture given by the formation itself. Each satellite will be equipped with an L-band interferometer and will behave as a node of a network to gain high-resolution images (up to 1-10 km) for land and oceans application. The SSO reference orbit has an altitude of 770 km, with a Local Time of the Ascending Node (LTAN) at 6 a.m.. The resulting nominal orbital parameters of the mission are reported in Table 1. A tight formation flying is designed around the virtual reference point on the orbit. The virtual plane of the formation is orthogonal to the orbital plane so that the semi-major axis of the three satellites is very similar. The position of the array can be described in the $(x, y, z)$ state in the orbital co-moving frame. The x-axis is in the direction of the reference orbit radius, the y-axis represents the curvilinear distance along the osculating orbit, and the z-axis is perpendicular to the reference orbit. The formation is planar, belonging to the $(y, z)$ plane, and distributed at the vertexes of a triangle, with the barycenter at the origin. It is assumed a virtual equilateral triangle with a side nominally equal to 13 m. The formation geometry is depicted in Figure 1. It can be observed that the satellites are close to each other, and they are not on a natural relative trajectory. The mission will require continuous control of the relative position to counteract any possible collision risk. Specifically, the propulsive system is selected to be a low thrust engine, with a maximum thrust available of 25 mN. The nominal condition of the formation is reported in Table 1. Its orientation in the TN plane is selected to have the same magnitude of natural oscillation in the normal direction for all the satellites. This results also in a balancing of the propellant consumption during the scientific mission operations.

**SSO Orbit**

| $a$ (km) | $e$ (-) | $i$ (deg) | $\Omega$ (deg) | $\omega$ (deg) |
|---|---|---|---|---|
| 7146 | 0 | 98.50 | 271 | 0 |

**FF nominal condition**

| | $x_R$ (m) | $x_T$ (m) | $x_N$ (m) |
|---|---|---|---|
| Sat 1 | 0 | 0 | -5.63 |
| Sat 2 | 0 | 6.5 | 5.63 |
| Sat 3 | 0 | -6.5 | 5.63 |

**Table 1**: Keplerian elements of the reference SSO orbit and relative position of the formation flying satellites in the RTN frame.

This paper focuses on the formation acquisition procedures after the orbit injection by the launcher. A fast reconfiguration was simulated as a preliminary analysis, to understand the limitation due to the propulsive system on-board. In the real scenario, a more relaxed constraint on the reconfiguration period will be simulated, to reduce even more the propellant consumption. The analysis was performed including both the mean $J_2$ and the control effect in the equation of motions. Then, the reconfiguration maneuver is modeled as a linear convex optimization subject to the dynamical constraints, with fixed initial and final conditions. The problem is manipulated to obtain a con-

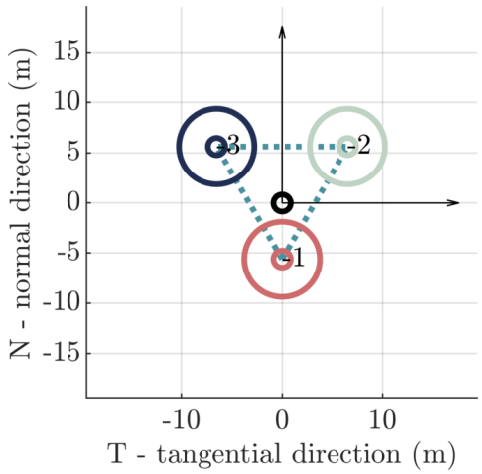


**Figure 1**: Geometry of the formation in the RTN reference frame.

vex description of the control problem. This approach is a quite common direct method to quickly solve an optimal control problem, by discretizing the system to obtain a finite-dimensional parameter optimization problem.[17,20] This approach is selected to include easily the fixed initial and final conditions for the reconfiguration in a fixed time interval, resulting in a simpler representation with respect to the classic linear programming approach.

## EQUATIONS OF MOTION

In literature, the limitation of the Clohessy-Wiltshire (C-W) equations has been widely discussed. Particularly, they introduce significant errors in the long-term prediction of the motion, especially for large inter-satellite separations. To account for these limitations, several models have been developed, which also allow the introduction of the effect of the earth's oblateness perturbation ($J_2$).[11,21,22] For this work, only the primary gravitational perturbation is considered, with no incorporation of drag or other perturbing effects. For the orbital condition defined in Table 1, the effects of drag and secondary perturbation can be reasonably neglected for the preliminary analysis. In this paper, the relative motion of the three satellites in the formation is described with respect to the reference point, nominally the geometric baricenter of the formation. This virtual point is described by the Keplerian orbital elements ($a$, $e$, $i$, $\Omega$, $\omega$, $M$), with $M$ the mean anomaly. The three satellites in the formation, identified as the Deputies, are expressed in ROEs and in the Hill Orbital Frame, which are also functions of the integration constants of the C-W equations in the Hill orbital frame.[9] The ROEs for each deputy are described as a set of dimensionless variables:

$$\delta\alpha = \begin{pmatrix} \delta a \\ \delta\lambda \\ \delta e_x \\ \delta e_y \\ \delta i_x \\ \delta i_y \end{pmatrix} = \begin{pmatrix} (a_d - a)/a \\ u_d - u + (\Omega_d - \Omega)\cos(i) \\ e_d cos(\omega_d) - e cos(\omega) \\ e_d sin(\omega_d) - e sin(\omega) \\ i_d - i \\ (\Omega_d - \Omega) sin(i) \end{pmatrix} \tag{1}$$

where $a$, $e$, $i$, $\Omega$, $\omega$ are the classical Keplerian elements, and $u = M + \omega$ is the mean argument of latitude, depending on the mean anomaly and on the argument of perigee. The ROEs are com-

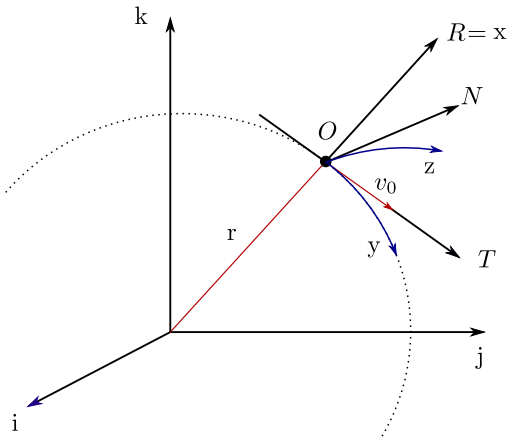


**Figure 2**: Hill Orbital system $(x, y, z)$ with respect to the Earth-Centred Inertial system $(i, j, k)$.

posed by the relative semi-major axis, the relative mean longitude and the relative eccentricity and inclination vectors respectively. In this representation, the chief satellite defines the origin of the Hill orbital frame, the local RTN frame. This is considered a curvilinear coordinate system defined by the unit vectors $[e_x, e_y, e_z]$. In this system the state of the three satellites is described by a vector $\mathbf{X} = (x, y, z, \dot{x}, \dot{y}, \dot{z})^T$, in the radial, transversal and normal direction respectively, as depicted in Figure 2. The relative motion under the effect of the mean $J_2$ is propagated through the ROE-based state transition matrix (STM).[10] Afterward, the relationship between the state X at the initial and current time is obtained using the linearized mean-to-osculating relationship and the first-order mapping into the Curvilinear reference frame provided by the geometric method of Gim and Alfriend.[21] Although these are known to introduce linearization errors,[10,23] for this preliminary study it is accepted. Note that this approximation affects the error in the initial conditions of the considered reconfiguration, that is when the satellites are far enough from each other. The geometric transformation between the RTN representation, $\mathbf{X}$ to the ROEs formulation $\delta\alpha$ is defined as:

$$\mathbf{X}(t) = \{A(t) + \kappa B(t)\}\delta\alpha(t), \tag{2}$$

where the coefficient $\kappa$ represents the contribution of the Earth Oblateness: $\kappa = 3J_2R_e^2$, with $R_e$ the radius of the Earth. Knowing the state transition matrix for the relative mean elements, $\delta\alpha(t) = \phi_\alpha\delta\alpha(t_0)$, it is possible to recover the relation for the relative dynamics in RTN frame:

$$\mathbf{X}(t) = \phi_{J_2}(t, t_0)\mathbf{X}(t_0) \tag{3}$$

where the state transition matrix $\phi_{J2}(t, t_0)$ for the relative motion is:

$$\phi_{J_2}(t, t_0) = \{A(t) + \kappa B(t)\}\phi_\alpha\{A(t_0) + \kappa B(t_0)\}^{-1} \tag{4}$$

The transformation matrix $\{A(t)+\kappa B(t)\}$ was computed with the approach in Gim and Alfriend.[21] The representation with the State Transition Matrix is computationally efficient with respect to a full integration of the dynamical system, since it requires the solution of the system at each time step, with no integration at all. This representation can be used only with linearized system dynamic, but can accurately approximate the non-linear motion of the system.[21] The Eq. (3), represents then the natural motion under the influence of the $J_2$ perturbation. The state transition matrix $\phi_{J_2}(t, t_0)$ can be in general described as a matrix $\mathbf{A}(t, t_0)$. Specifically, this matrix could be derived from a more complex dynamic to include also the secondary order perturbing effect on the satellite motion.

## LOW THRUST OPTIMAL MANEUVER

The satellites in the formation are equipped with a low thrust propulsive system, which provides the control term during the whole mission via continuous acceleration. This control is introduced in the dynamical system as a continuous effect on the natural dynamics. The control term is described in the RTN relative frame as a control input: $\mathbf{u}(t) = (u_x(t), u_y(t), u_z(t))^T$. The continuous control is typically introduced in the dynamical system as a integral term, affecting the velocity components of the state vector:

$$\mathbf{X}(t) = \mathbf{A}(t, t_0)\mathbf{X}(t_0) + \int_t \mathbf{B}\mathbf{u}(t)\, dt \tag{5}$$

with $\mathbf{A}(t, t_0)$ the generic matrix describing the natural dynamics of the system under the effect of the $J_2$ perturbation. The control input matrix $\mathbf{B}$ is introduced to correctly relate the control term to the velocity components of $\mathbf{X}$:

$$\mathbf{B} = \begin{pmatrix} 0 & 0 & 0 \\ 0 & 0 & 0 \\ 0 & 0 & 0 \\ 1 & 0 & 0 \\ 0 & 1 & 0 \\ 0 & 0 & 1 \end{pmatrix} \tag{6}$$

In this paper, both the satellite state $\mathbf{X}(t)$ and the acceleration vector $\mathbf{u}(t)$ are known only at the initial and final conditions. The initial condition is given by the formation flying condition after the orbit insertion and commissioning phase. At this point a reconfiguration maneuvre is required by the propulsive system. In this paper, the motion is discretized in time to include the control term in the STM representation, as described in the following. The discretization of the system is the first step to write an optimal control problem in convex form. Specifically, the convexification of the problem aims to obtain a system with a unique optimal solution. The approach followed for discretizing the system is similar to the one introduced for the system dynamics in the relative RTN frame in literature.[22] This representation allows a simple immediate discretization of the system dynamic, including the effect of the control action. The discretization of the system in K time instants is reduced to

$$x^{k+1} - \mathbf{A}^k x^k - \Delta t \mathbf{B} u^k = 0, \qquad k = 1, ..., K-1. \tag{7}$$

### Reconfiguration as a constrained optimal problem

The reconfiguration maneuver can be described as a time-optimal or a fuel-optimal problem. In this case, the approach was to fix the time for the reconfiguration and optimize propellant consumption. The following control problem was considered:

$$\begin{aligned} &\text{minimze}: \qquad \mathcal{J}(u(t)) := \int_0^{t_f} ||u_j(t)|| dt, \\ &\text{subject to}: \quad \dot{\mathbf{x}}_j(t) = \mathbf{A}(t, t_0)\mathbf{X}_j(t) + \int_t \mathbf{B}\mathbf{u}_j(t)\, dt; \quad \mathbf{x}_j(t_0) = \mathbf{x}_{j0}; \\ &\qquad\qquad \mathbf{x}_j(t_f) = \mathbf{x}_{jf}; \qquad ||\mathbf{u}_j(t)|| \leq T_{max}; \end{aligned} \tag{8}$$

where the cost function $\mathcal{J}(u(t))$ was selected to minimize the control effort, $t_0$ and $t_f$ are the initial and final time respectively, and $T_{max}$ is the maximum thrust available from the propulsive

system. The constraints include the system dynamic for each satellite, with $j = 1, ..., 3$. The initial and final state of each satellite is imposed in the optimization, as well as the control effort, which should not exceed the maximum thrust available by the propulsive system. Moreover, due to the minimum allowable distance between the satellite, a collision-avoidance condition is implemented and verified after the optimization. Now, the problem is manipulated into a convex form. This requires the discretization of the entire control problem, for both constraints and cost function. The following conditions were considered in the convexification procedure:

$$\text{No. of satellites}: \quad j = 1, ..., N; \ (N = 3) \tag{9}$$

$$\text{Time discretization}: \quad k = 1, ..., K. \tag{10}$$

For each satellite $j$, the state is a $(6K + 3(K - 1))$ column vector $\mathbf{x}_j$ containing the position, the velocity, and the control vector at each time instant $k$:

$$\hat{\mathbf{x}}_j = \begin{pmatrix} \mathbf{x}_j^1 & ... & \mathbf{x}_j^k & ... & \mathbf{x}_j^K & \mathbf{u}_j^1 & ... & \mathbf{u}_j^k & ... & \mathbf{u}_j^{K-1} \end{pmatrix}^T \tag{11}$$

For the whole formation ($j = 1, ..., N$), the full state is a $N(6K + 3(K - 1))$ column vector $\mathcal{Z}$:

$$\mathcal{Z} = \begin{pmatrix} \hat{\mathbf{x}}_1 & \hat{\mathbf{x}}_2 & \hat{\mathbf{x}}_3 \end{pmatrix}^T \tag{12}$$

For conciseness, we define the length of the decisional vector for the generic satellite $j$ as $M = 6K + 3(K - 1)$. Now the *cost function* is written as:

$$\mathcal{J} = \text{norm}(\hat{\mathbf{H}} \mathcal{Z} \, \Delta t) \tag{13}$$

where $\Delta t$ is the time step of the discretization: $\Delta t = t^{k+1} - t^k$, while the $\hat{\mathbf{H}}$ is chosen as a $(N \cdot M)$ square matrix to extract only the control terms from the decisional vector $\mathcal{Z}$:

$$\hat{\mathbf{H}} = \begin{bmatrix} ... & ... & ... \\ \mathbf{0}_{M \times M(j-1)} & \mathbf{H} & \mathbf{0}_{M \times M(N-j)} \\ ... & ... & ... \end{bmatrix} \qquad \forall j = 1, .., N \tag{14}$$

And the matrix $\mathbf{0}$ is defined as $(M)$ null square matrix, apart from the components to extract the control term $\mathbf{u}$:

$$\mathbf{H}(6K + 1 : M, 6K - 1 : M) = \begin{bmatrix} I_{3(K-1)} \end{bmatrix} \tag{15}$$

where the $I_{3(K-1)}$ is the identity matrix of dimensions $3(K - 1)$. With the same procedure, the *system dynamics*, the *initial conditions* and the *final conditions* are expressed as:

$$\hat{\mathbf{A}}_{sd} \mathcal{Z} = \mathbf{0} \tag{16}$$

$$\hat{\mathbf{A}}_0 \mathcal{Z} = \mathbf{X}_0 \tag{17}$$

$$\hat{\mathbf{A}}_f \mathcal{Z} = \mathbf{X}_f \tag{18}$$

For the *system dynamics*, $\hat{\mathbf{A}}_{sd}$ is a $(6N(K - 1) \times N \cdot M)$ matrix defined as:

$$\hat{\mathbf{A}}_s d = \begin{bmatrix} ... & ... & ... \\ \mathbf{0}_{M \times M(j-1)} & \mathbf{A}_{sd} & \mathbf{0}_{M \times M(N-j)} \\ ... & ... & ... \end{bmatrix} \qquad \forall j = 1, .., N \tag{19}$$

where $\mathbf{A}_{sd}$ is a $(6(K-1) \times M)$ matrix which includes the dynamical behaviour for the satellite $j$ in the FF:

$$\mathbf{A}_{sd} = \begin{bmatrix} ... & ... & ... & & & \\ \mathbf{0}_{6\times 6(K-1)} & -\mathbf{A}(t_k) & \mathbf{I}_6 & \mathbf{0}_{6\times 6K+3(k-3)} & -\Delta\mathbf{B} & \mathbf{0}_{6\times 3(K-k-1)} \\ ... & ... & ... & & & \end{bmatrix} \qquad \forall j = 1, .., N \tag{20}$$

For the *initial condition*, $\hat{\mathbf{A}}_0$ is a $(6N(K-1) \times N\,M)$ matrix defined as:

$$\hat{\mathbf{A}}_0 = \begin{bmatrix} ... & ... & ... \\ \mathbf{0}_{M\times M(j-1)} & \mathbf{A}_0 & \mathbf{0}_{M\times M(N-j)} \\ ... & ... & ... \end{bmatrix} \qquad \forall j = 1, .., N \tag{21}$$

where $\mathbf{A}_0$ is a $(6(K-1) \times\ M)$ matrix which includes the dynamical behaviour for the satellite $j$ in the FF. While $X_0$ is defined as a $(N \cdot 6K)$ column vector:

$$X_0 = \begin{bmatrix} x_1^0 & ... & x_j^0 & ... & x_N^0 \end{bmatrix} \tag{22}$$

to impose both initial condition on the relative position and velocity. For the *final condition*, $\hat{\mathbf{A}}_f$ is a $(6N(K-1) \times N\,M)$ matrix defined as:

$$\hat{\mathbf{A}}_f = \begin{bmatrix} ... & ... & ... \\ \mathbf{0}_{M\times M(j-1)} & \mathbf{A}_f & \mathbf{0}_{M\times M(N-j)} \\ ... & ... & ... \end{bmatrix} \qquad \forall j = 1, .., N \tag{23}$$

where $\mathbf{A}_f$ is a $(6(K-1) \times M)$ matrix which includes the dynamical behaviour for the satellite $j$ in the FF. while $X_f$ is defined as a $(N \cdot 6K)$ column vector:

$$X_f = \begin{bmatrix} x_1(t_K) & ... & x_j(t_K) & ... & x_N(t_K) \end{bmatrix} \tag{24}$$

to impose both initial condition on the relative position and velocity. Finally, the *maximum available thrust* is imposed with the convex form:

$$\hat{\mathbf{A}}_t \mathcal{Z} \leq T_{max} \mathbf{I}_{6N(K-1)\times 1} \tag{25}$$

In this case, the matrix $\hat{\mathbf{A}}_t$ is defined for the case of multiple thruster, i.e. each satellite could provide a thrust in a generic direction along the $(x, y, z)$ relative orbital frame. This matrix is given by:

$$\hat{\mathbf{A}}_t = \begin{bmatrix} ... & ... & ... \\ \mathbf{0}_{M\times M(j-1)} & \mathbf{A}_t & \mathbf{0}_{M\times M(N-j)} \\ ... & ... & ... \end{bmatrix} \qquad \forall j = 1, .., N \tag{26}$$

where the matrix for the maximum thrust is defined as $\mathbf{A}_t = [\tilde{\mathbf{A}}_t; -\tilde{\mathbf{A}}_t]$, as

$$\tilde{\mathbf{A}}_t(:, 6K+1 : M) = \mathbf{I}_{3(K-1)} \tag{27}$$

Finally, the collision avoidance is implemented starting from the minimum inter-satellite distance allowed before the collision among two pair of satellites happens. The condition is recovered from the requirement that $||x_j^k - x_l^k||^2 \geq R_{coll}^2$, with $j, l$ the indexes of a pair of satellite of the FF and the

$R_{coll}$ the minimum inter-satellite distance margined by $20\%$. The convex form of this requirement is implemented as

$$\hat{\mathbf{A}}_{ca}\mathcal{Z} \geq R_{coll}^2 \mathbf{I}_{6NK\times 1} \tag{28}$$

where the matrix $\hat{\mathbf{A}}_{ca}$ is defined depending on the formation geometry and current state. In our case, it is given by

$$\hat{\mathbf{A}}_{ca} = \begin{bmatrix} \mathbf{A}_{ca} & \mathbf{0}_{6K,3(K-1))} & -\mathbf{A}_{ca} & \mathbf{0}_{6K,6(2K-1))} & \dots \\ \mathbf{A}_{ca} & \mathbf{0}_{6K,6(2K-1))} & \dots & -\mathbf{A}_{ca} & \mathbf{0}_{6K,3(K-1))} \\ \mathbf{0}_{6K,3(K-1)+6K)} & \mathbf{A}_{ca} & \mathbf{0}_{6K,3(K-1))} & -\mathbf{A}_{ca} & \mathbf{0}_{6K,3(K-1))} \end{bmatrix} \tag{29}$$

The matrix $\mathbf{A}_{ca}$ is chosen to extract from the state vector $\mathcal{Z}$ the component $x_j^k$. After that, the equations are turned into their convex form, and the new optimal control problem is reformulated as follows:

$$\begin{aligned} \text{minimze}: \quad & \mathcal{J}(u(t)) := norm((\hat{\mathbf{H}}\mathcal{Z})\Delta t), \\ \text{subject to}: \quad & \hat{\mathbf{A}}_{sd}\mathcal{Z} = \mathbf{0}; \quad \hat{\mathbf{A}}_0\mathcal{Z} = \mathbf{X}_0; \\ & \hat{\mathbf{A}}_f\mathcal{Z} = \mathbf{X}_f; \quad \hat{\mathbf{A}}_t\mathcal{Z} \leq T_{max}\mathbf{I}_{6N(K-1)\times 1}; \\ & \hat{\mathbf{A}}_{ca}\mathcal{Z} \geq R_{coll}^2 \mathbf{I}_{6NK\times 1} \end{aligned} \tag{30}$$

This problem was implemented in MATLAB® and to solve convex optimization problem, we used CVX, a package for specifying and solving convex programs.[24,25] The CVX supports diciplined convex programming, where constraints and objectives are automatically transformed in canonical form and solved.

## MISSION DESIGN: INITIAL PHASE PRELIMINARY RESULTS

This section presents the results of the analysis for the initial phase design, from the orbit injection to the formation reconfiguration of the mission, described in Section *Mission Overview*.

### Orbit injection

The three satellites are launched together with a single launch, and the separation procedure is planned as follows. The final stage of the launcher brings the satellites on the nominal SSO orbit (see Table 1), and then imparts a separation velocity of 1 m/s to each satellite in the transversal – along-track – direction. Note that for this study the direction of ejection of the satellites from the carrier is determined by the typical operation strategy adopted by launcher providers and therefore is not a degree of freedom of the problem. This is a substantial difference with respect to in-orbit formation establishment[26] or envisioned for swarm deployment.[8] The time separation between each satellite at the deployment is 10 s. After the injection, due to the velocity separation, the satellites are on an orbit very close to the SSO nominal orbit, with a separation mainly in the argument of latitude. The RTN relative position and velocity imparted by the launcher to each spacecraft is $[0, 0, 0, 0, 1, 0]^T$ (m/s). The situation just after the injection is reported in Figure 3. Both conditions in the RTN and ROEs frame are depicted considering the satellite 1 as the reference satellites, nominally the first one released by the launcher. It shows that the time separation in the deployment is enough to guarantee a good separation in $\delta\lambda$ and in $\delta e_y$. In the case under analysis, the launcher provides a delta-v in the tangential direction of 1 m/s every 10 s, to ensure the safe separation among the satellites. Increasing the time separation results also to an increase of the spatial separation, increasing the safety of the deployment but posing more challenges to the successful establishment of the nominal FF geometry. The corresponding RTN and ROEs elements are shown in Figure 4.

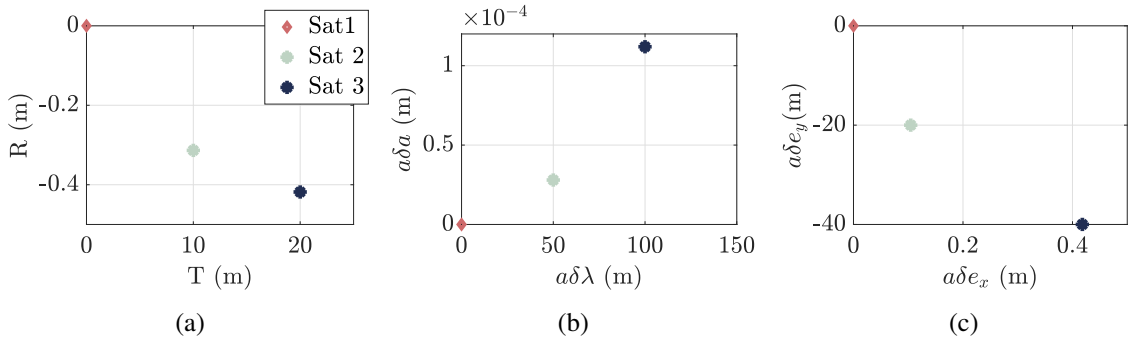


**Figure 3**: Initial condition after orbit injection by the launcher with 10 s time separation (Satellite 1 is taken as the reference). RT-plane relative condition (a) and ROEs (b, c).

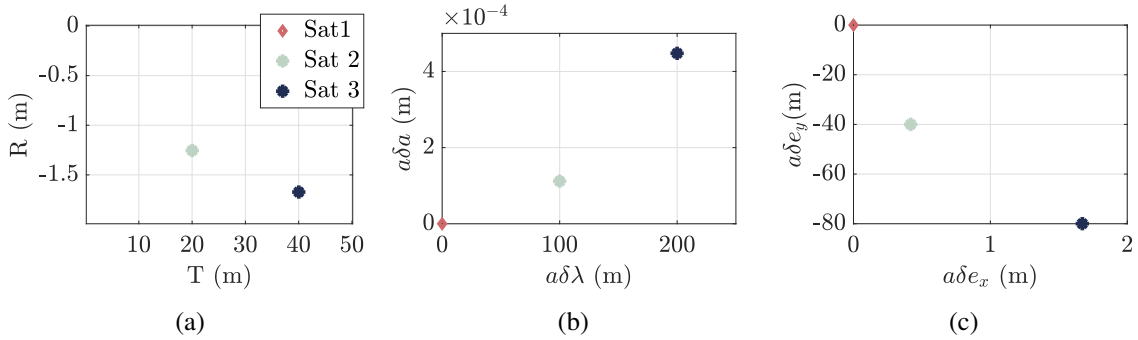


**Figure 4**: Initial condition after orbit injection by the launcher with 20 s time separation (Satellite 1 is taken as the reference). RT-plane relative condition (a) and ROEs (b, c).

### Commissioning phase

Once the three satellites are placed on their initial orbit, the commission phase is necessary to perform the preliminary tests on the satellite subsystem and components: the calibration/validation of each onboard instrument is performed. In this scenario, a preliminary analysis is considered without the use of the low-thrust continuous control profile, assuming a natural evolution of the satellites under the effect of the orbital perturbations. Two main scenarios are investigated. A first scenario considers a short commissioning phase, up to 1 month. A second scenario, instead, analyses the commissioning for a much longer period, up to 6 months The satellites' initial conditions were simulated with a high fidelity propagator, to accurately simulate the real behavior of the system under the orbital perturbations.

The final conditions to the satellite 1 are reported in Figure 5. Moreover, the final Keplerian elements for each satellite are reported in Table 2. It can be seen that the natural evolution brings the satellites to increase the separation to the reference orbit. Specifically, the $J_2$ effect is evident on the semi-major axis, the eccentricity of the orbits, causing in time an increase of the eccentricity and a decrease of the semi-major axis. Moreover, the drift in the right ascension of the ascending node is present under the effect of the $J_2$ perturbation. The propagation was performed with a high fidelity propagator (i.e. GMAT software) including the most important perturbations. The variation underlined in Table 2 results in a higher propulsive effort for a longer commissioning phase. This

is valid under the hypothesis of considering a fixed time interval available for the reconfiguration of the formation. In this way, we investigate the feasibility of a fast reconfiguration to understand the limitation of the low thrust propulsive system for a quick maneuver time.

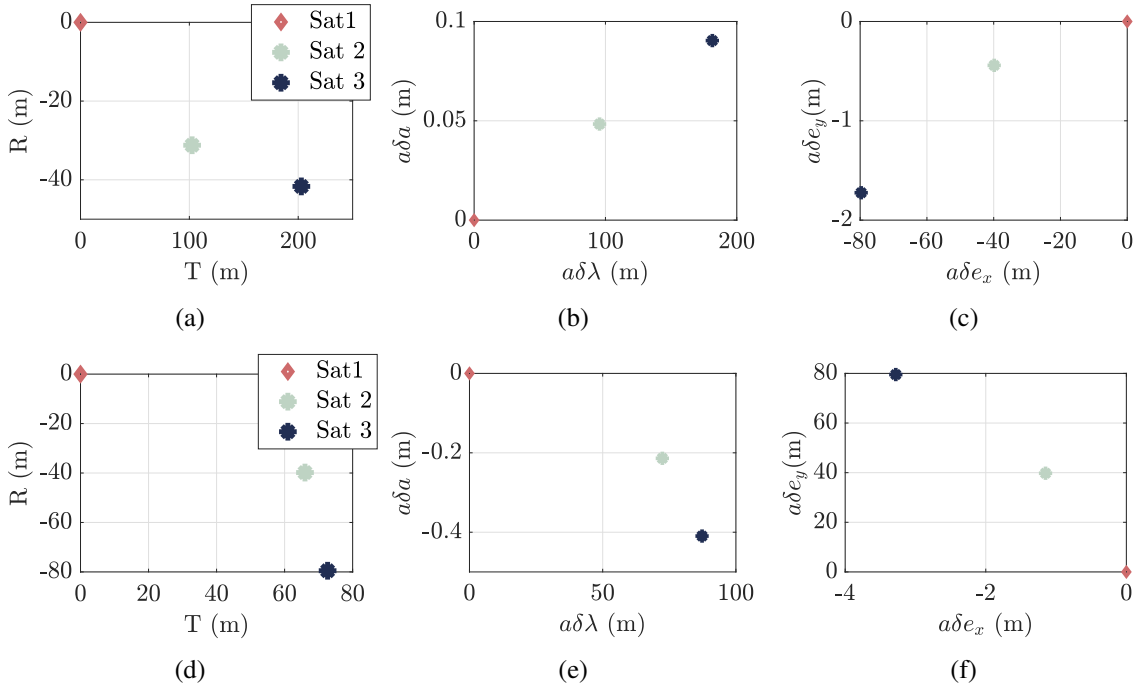


**Figure 5**: RTN and ROEs condition after commissioning phase, for 1 month propagation (case 1: a,b) and 6 month propagation (case 2: c,d). The relative elements for both RTN and ROEs frame are recover for satellite 2 and 3 with respect to satellite 1.

| | $a$ (km) | $e$ (-) | $i$ (deg) | $\Omega$ (deg) | $\omega$ (deg) | $M$ (deg) |
|---|---|---|---|---|---|---|
| | | | Case 1 | | | |
| Sat 1 | 7145.07 | $7.8387e-4$ | 98.50 | 300.89 | 295.52 | 50.96 |
| Sat 2 | 7145.07 | $7.8154e-4$ | 98.50 | 300.89 | 295.15 | 51.33 |
| Sat 3 | 7145.07 | $7.7934e-4$ | 98.50 | 300.89 | 294.77 | 51.71 |
| | | | Case 2 | | | |
| Sat 1 | 7128.02 | 0.001807 | 98.51 | 89.94 | 2.52 | 195.48 |
| Sat 2 | 7128.02 | 0.001802 | 98.51 | 89.93 | 2.52 | 195.54 |
| Sat 3 | 7128.02 | 0.001796 | 98.51 | 89.94 | 2.51 | 195.61 |

**Table 2**: Final Keplerian elements of the satellites after the commissioning phase. Case 1 identifies the commissioning of 1 month, while case 2 identifies the commissioning of 6 month.

**Formation reconfiguration strategy**

The strategy for the formation reconfiguration presented in this section aims at estimating the propulsive effort for a quick maneuver. Specifically, a rapid reconfiguration is assumed to happen in one orbital period. One comment is necessary for this assumption. During the real mission operations, and typically after the commissioning, it is not required to have a fast reconfiguration. Nominally this situation could also last several days to save propellant. This work wants to investigate the limitation of a fast reconfiguration to assess a limit in the propellant consumption needed for establishing the formation. The formation initial and final condition, after the commissioning phase and during the nominal operations respectively, are shown in Table 2 and 1. The condition in RTN is computed from the ROEs elements, considering the curvilinear reference frame. The chief elements are reported in Table 1. The simulation assumes a total reconfiguration in 1 orbital period for the three satellite systems, with a discretization of $0.5°/n$ deg on the orbit. Hence the final time is taken as $t_f = 360°/n$ with $n$ the reference orbit mean motion. Furthermore, a safety distance margined by $20\%$ was considered to maintain the satellites at least to a $10$ m distance.

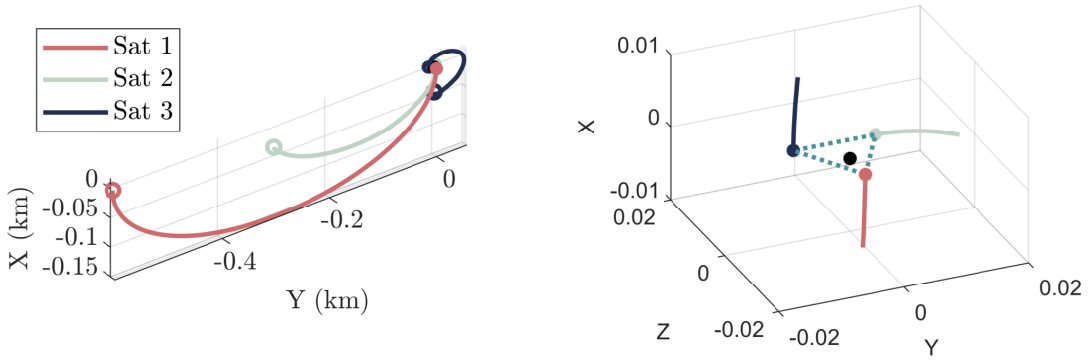


(a) (b)

**Figure 6**: Reconfiguration trajectory for the case 1 (1 month commissioning).

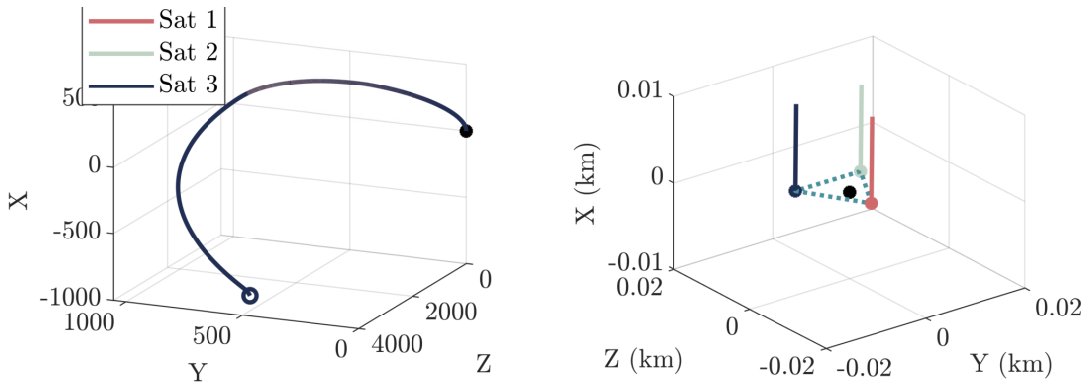


(a) (b)

**Figure 7**: Reconfiguration trajectory for the case 2 (6 month commissioning).

Figure 6 and 7 show the reconfiguration strategy for the two cases presented in the section *Commissioning phase*. For the second case, with a longer commissioning phase, the satellites are farther from the virtual reference point. For this reason, they will follow a very similar trajectory. Figure 8 represents the relative trajectory of satellite 2 and 3 respect to satellite 1 to appreciate the different trajectory followed. In these figures, the filled marker represents the target final position. The other marker instead, represents the initial condition before the reconfiguration maneuver. The initial separation with respect to the reference orbit is much more evident in the second case since the six-month commissioning produces a higher variation in the semi-major axis and eccentricity of the orbits. The satellites are reconfigured in a triangular formation, as shown in Figure 6-b and 7-b, around the reference virtual point on the nominal SSO orbit.

The collision avoidance is satisfied in both cases, as depicted in Figure 9 and Figure 10. Those figures represent the spacecraft inter-satellite distance. It is shown how for the entire formation reconfiguration, the satellites stay at more than 10 m from each other. Moreover, this stringent condition is reached only at the final steps of the reconfiguration, when the formation tends to the nominal case, with a final inter-satellite distance of 13 m.

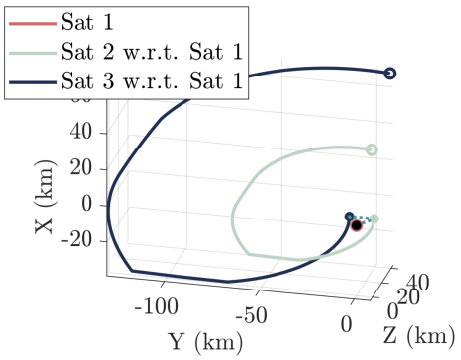


**Figure 8**: Reconfiguration trajectory for the case 2 (6 month commissioning). The relative trajectory of satellites 2 and 3 are here represented with respect to the trajectory of satellite 1.

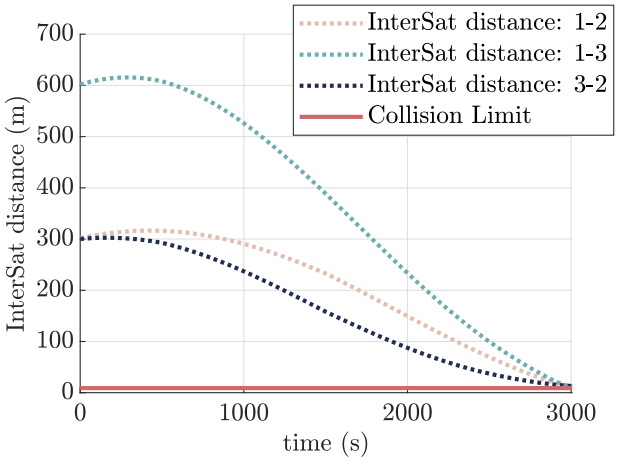


**Figure 9**: Inter-satellite distance evaluation during the reconfiguration manoeuvre (1 month commissioning).

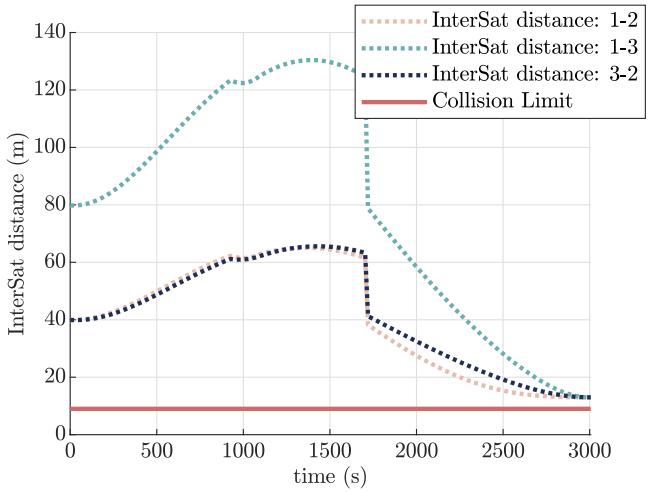


**Figure 10**: Inter-satellite distance evaluation during the reconfiguration manoeuvre (6 month commissioning).

Finally, also the maneuvering plan is shown in Figure 11 and 12. In both cases, the maneuvering plans provide an optimal strategy to correct at a certain time instant the trajectory, saving propellant. In the first case, the satellites are positioned around the reference point such that the trajectory followed is quite different, and this results in a control strategy different for each satellite. In this case, the delta-v required by each satellites for the reconfiguration is respectively $[0.9591 \quad 0.5925 \quad 1.790]$ mm/s. On the other hand, in the second case, it was shown that the trajectory followed is very similar. The maneuvering plan is almost equal among the satellites. This second condition requires a delta-v of 5.7361 m/s for the reconfiguration.

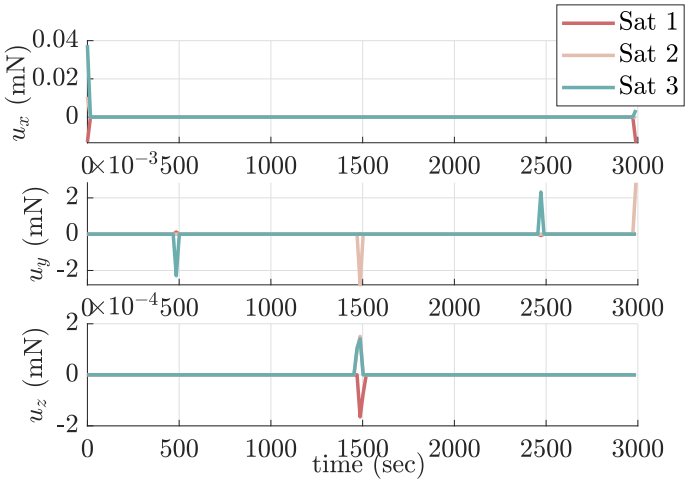


**Figure 11**: Maneuvring plan evaluation for each satellite during the reconfiguration maneuvre (1 month commissioning).

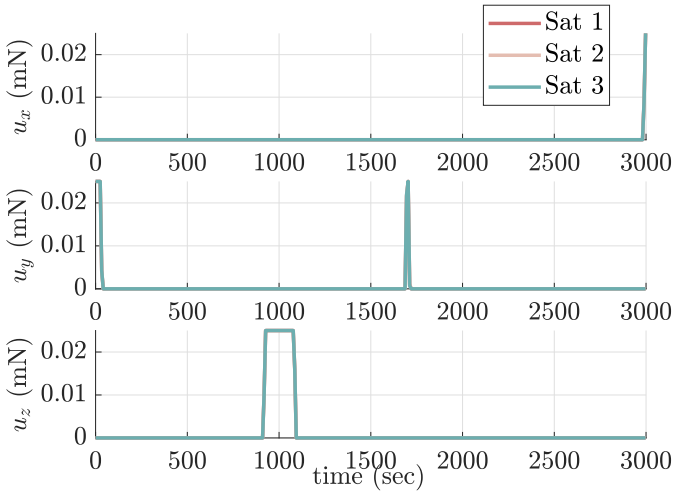


**Figure 12**: Maneuvring plan evaluation for each satellite during the reconfiguration maneuvre (6 month commissioning).

## CONCLUSION

In this paper, we show a fast approach to reconfigure a satellite formation after the orbital injection. The maneuvering plan is defined via the optimization of the control problem in the convex form. This methodology allows a fast resolution of the system ($\sim$ 3 s for both cases presented), by discretizing the problem in relatively few time instant. Moreover, the methodology applied, ensures the application of a delta-v only at optimal time instants, saving propellant consumption. In the first framework, the results provide a fast and cheap reconfiguration, since, in a short commissioning phase, the difference in relative orbital parameters is small. On the other hand, the second case presented, implements a quite higher delta-v, this is mainly due to the constraint given on the longer duration of the commissioning time. A fast reconfiguration is more expensive due to the more significant difference among the satellite elements and the reference orbit ones.

In both cases, the reconfiguration problem is approached as a minimization problem. The cost function aims to minimize the total delta-v for the maneuvers. The explicit derivation of the constraint from the system dynamics, initial conditions, and final conditions support the software implementation of the proposed strategy. A convex approach is computationally less expensive than an optimization including the integration of the dynamics at each time step. This could also be envisioned as a proper method to be put in the on-board software for formation maneuver implementation. Moreover, the concept of a fast maneuver could be applied to formation maneuvers during the nominal mission phase, such as for the safety maneuver to switch to safe mode or to implement a maneuver just after a possible failure in the system.

Further development of the methodology will include the uncertainties after the launcher injection in the semi-major axis and the inclination. This will be managed with a Monte Carlo simulation to generate the initial condition for the formation reconfiguration to the solver.

## ACKNOWLEDGMENT

The project presented in this paper was carried out as part of the European Space Agency Contract (Contract No. 4000128576/19). The view expressed in this paper can in no way be taken to reflect

the official opinion of the European Space Agency.
The work was co-founded by the European Space Agency (Contract No. 4000128576/19) and by the European Research Council (ERC) under the European Unions Horizon 2020 research and innovation program (grant agreement No. 679086 COMPASS).
The contribution of Dr. Gabriella Gaias is funded by the European Union's Horizon 2020 research and innovation program under the Marie-Sklodowska Curie grant ReMoVE (grant agreement No. 793361).
The authors acknowledge the contribution of Dr. Berthyl Duesmann and Dr. Itziar Bara, orbital experts at ESA European Space Research and Technology Centre (ESTEC).
The authors also would like to acknowledge Dr. Miguel Piera's support, from Airbus Space España, leading the contract.

## REFERENCES

[1] G. Krieger, A. Moreira, H. Fiedler, I. Hajnsek, M. Werner, M. Younis, and M. Zink, "TanDEM-X: A satellite formation for high-resolution SAR interferometry," *IEEE Transactions on Geoscience and Remote Sensing*, Vol. 45, No. 11, 2007, pp. 3317–3341, https://doi.org/10.1109/TGRS.2007.900693.

[2] S. Bandyopadhyay, R. Foust, G. P. Subramanian, S.-J. Chung, and F. Y. Hadaegh, "Review of formation flying and constellation missions using nanosatellites," *Journal of Spacecraft and Rockets*, Vol. 53, No. 3, 2016, pp. 567–578, https://doi.org/10.2514/1.A33291.

[3] A. M. Zurita, I. Corbella, M. Martín-Neira, M. A. Plaza, F. Torres, and F. J. Benito, "Towards a SMOS operational mission: SMOSOps-hexagonal," *IEEE Journal of Selected Topics in Applied Earth Observations and Remote Sensing*, Vol. 6, No. 3, 2013, pp. 1769–1780, https://doi.org/10.1109/JSTARS.2013.2265600.

[4] Y. H. Kerr, A. Al-Yaari, N. Rodriguez-Fernandez, M. Parrens, B. Molero, D. Leroux, S. Bircher, A. Mahmoodi, A. Mialon, P. Richaume, *et al.*, "Overview of SMOS performance in terms of global soil moisture monitoring after six years in operation," *Remote Sensing of Environment*, Vol. 180, 2016, pp. 40–63, https://doi.org/10.1016/j.rse.2016.02.042.

[5] E. S. Agency, "Summary on "ECMWF/ESA workshop on using low frequency passive microwave measurements in research and operational applications"," 2017.

[6] M. Martin-Neira, "SMOS Follow-on - H," *L-band Continuation Workshop, CESBIO, Toulouse (France)*, 28-30 November 2018.

[7] M. Martin-Neira, A. M. Zurita, M. A. Plaza, and F. J. Benito, "SMOS Follow-on Operational Mission Concept (SMOSops-H)," *2nd SMOS Science Conference, ESAC, Villanueva de la Cañada*, 25-29 May 2015.

[8] A. W. Koenig and S. D'Amico, "Safe spacecraft swarm deployment and acquisition in perturbed near-circular orbits subject to operational constraints," *Acta Astronautica*, Vol. 153, 2018, pp. 297–310, https://doi.org/10.1016/j.actaastro.2018.01.037.

[9] S. D'Amico, "Relative orbital elements as integration constants of Hill's equations," *DLR, TN*, 2005, pp. 05–08.

[10] G. Gaias, C. Colombo, and M. Lara, "Analytical Framework for Precise Relative Motion in Low Earth Orbits," *Journal of Guidance, Control, and Dynamics*, Vol. 43, No. 5, 2020, pp. 915–927, https://doi.org/10.2514/1.G004716.

[11] M. Sabatini and G. B. Palmerini, "Linearized Formation-Flying Dynamics in a Perturbed Orbital Environment," *2008 IEEE Aerospace Conference*, 2008, pp. 1–13, https://doi.org/10.1109/AERO.2008.4526271.

[12] C. Wei, S.-Y. Park, and C. Park, "Linearized dynamics model for relative motion under a J2-perturbed elliptical reference orbit," *International Journal of Non-Linear Mechanics*, Vol. 55, 2013, pp. 55–69, https://doi.org/10.1016/j.ijnonlinmec.2013.04.016.

[13] S. Vaddi, K. T. Alfriend, S. Vadali, and P. Sengupta, "Formation establishment and reconfiguration using impulsive control," *Journal of Guidance, Control, and Dynamics*, Vol. 28, No. 2, 2005, pp. 262–268, https://doi.org/10.2514/1.6687.

[14] M. Chernick and S. D'Amico, "New closed-form solutions for optimal impulsive control of spacecraft relative motion," *Journal of Guidance, Control, and Dynamics*, Vol. 41, No. 2, 2018, pp. 301–319, https://doi.org/10.2514/1.G002848.

[15] G. Gaias and S. D'Amico, "Impulsive maneuvers for formation reconfiguration using relative orbital elements," *Journal of Guidance, Control, and Dynamics*, Vol. 38, No. 6, 2015, pp. 1036–1049, https://doi.org/10.2514/1.G000189.

[16] S. Mitani and H. Yamakawa, "Continuous-thrust transfer with control magnitude and direction constraints using smoothing techniques," *Journal of guidance, control, and dynamics*, Vol. 36, No. 1, 2013, pp. 163–174, https://doi.org/10.2514/1.56882.

[17] S. Sarno, J. Guo, M. D'Errico, and E. Gill, "A guidance approach to satellite formation reconfiguration based on convex optimization and genetic algorithms," *Advances in Space Research*, 2020, https://doi.org/10.1016/j.asr.2020.01.033.

[18] L. M. Steindorf, S. D'Amico, J. Scharnagl, F. Kempf, and K. Schilling, "Constrained low-thrust satellite formation-flying using relative orbit elements," *27th AAS/AIAA Space Flight Mechanics Meeting*, 2017.

[19] P. M. Pardalos, "Convex optimization theory," *Optimization Methods and Software*, Vol. 25, No. 3, 2010, pp. 487–487, https://doi.org/10.1080/10556781003625177.

[20] B. Acikmese, D. Scharf, F. Hadaegh, and E. Murray, "A convex guidance algorithm for formation reconfiguration," *AIAA Guidance, Navigation, and Control Conference and Exhibit*, 2006, p. 6070.

[21] D.-W. Gim and K. T. Alfriend, "State transition matrix of relative motion for the perturbed noncircular reference orbit," *Journal of Guidance, Control, and Dynamics*, Vol. 26, No. 6, 2003, pp. 956–971.

[22] D. Izzo, M. Sabatini, and C. Valente, "A new linear model describing formation flying dynamics under J2 effects," *Proceedings of the 17th AIDAA National Congress*, Vol. 1, 2003, pp. 15–19.

[23] G. Gaias, J.-S. Ardaens, and C. Colombo, "Precise Line-of-Sight Modelling for Angles-Only Relative Navigation," *Advances in Space Research, Article in Advance (published online 10 Jun 2020)*, Vol. ISSN 0273-1177, 2020, https://doi.org/10.1016/j.asr.2020.05.048 (open access).

[24] M. C. Grant and S. P. Boyd, "Graph implementations for nonsmooth convex programs," *Recent advances in learning and control*, pp. 95–110, Springer, 2008.

[25] M. Grant, S. Boyd, and Y. Ye, "CVX: Matlab software for disciplined convex programming, version 2.0 beta," 2013.

[26] M. Wermuth, G. Gaias, and S. D'Amico, "Safe Picosatellite Release from a Small Satellite Carrier," *Journal of Spacecraft and Rockets*, Vol. 52, No. 5, 2015, pp. 1338–1347, 10.2514/1.A33036.